DOI: 10.1017/S1431927603442050
Microsc Microanal 9(Suppl 2), 2003


# CTEM, HRTEM and FE-AEM Investigation of the Metastable Tetragonal Phase Stabilization in Undoped, Sol-Gel Derived, Nanocrystalline Zirconia

Vladimir P. Oleshko[*], James M. Howe[*], Satyajit Shukla[**], Sudipta Seal[**]

[*]University of Virginia, Department of Materials Science & Engineering, Charlottesville, VA 22904
[**]University of Central Florida, Advanced Materials Processing and Analysis Center & Mechanical Materials Aerospace Engineering Department, Orlando, Florida 32816.

Stabilizing the metastable *t*-phase in $ZrO_2$ powders is a major challenge and dopants are usually used [1]. In this paper, the mechanisms underlying stabilization of the *t*-phase in undoped, sol-gel derived nanocrystalline $ZrO_2$ are studied by conventional and high-resolution transmission electron microscopy (CTEM/HRTEM) combined with field-emission analytical electron microscopy (FE-AEM) utilizing parallel electron energy-loss spectroscopy (PEELS). $ZrO_2$ nanopowders were synthesized by hydrolysis of zirconium (IV) n-propoxide in an alcohol solution at two ratios of molar concentrations of water to zirconium n-propoxide, R=5 and 60, in the presence of 1.0 g/L hydroxylpropyl cellulose. The sol was subsequently dried at 80$^o$C following calcination of a gel for 2 h at 400$^o$C in air. Samples were examined using bright-field (BF) and dark-field (DF) TEM, selected-area electron diffraction (SAED) and HRTEM in a JEOL 4000EX TEM operating at 400 kV and in a JEOL 2010F FE-AEM operating at 200 kV and equipped with a Gatan Model 678 Imaging Filter. The as-precipitated $ZrO_2$ processed with R=5 contained highly aggregated clusters and elongated denser particles 200-500 nm in diameter. HRTEM examination, however, revealed nanocrystals 5-11 nm in size, randomly distributed in the amorphous matrix (Fig. 1a) that could serve as nuclei for growing crystalline phases during calcination. In contrast, calcinated $ZrO_2$ particles 400-600 nm in size, were found to be highly crystalline as indicate distinct Bragg reflections assigned to the *t*-phase in a SAED pattern (insert in Fig. 1b). DF TEM using the $\bar{1}0\bar{1}$ reflection showed 10-100 nm–sized crystalline regions of various shapes throughout the particles. Multiple lattice fringes with spacings ~0.25-0.64 nm were observed by HRTEM (Fig. 1c). The $ZrO_2$ powder precipitated at R=60 consisted of 4-11 nm-sized particles forming aggregates (~50-100 nm) with an amorphous structure (Fig. 2a). The SAED pattern (insert in Fig. 2a) shows a broad diffuse ring with an intensity maximum corresponding to the most probable interatomic spacing ~ 0.3 nm. BF TEM (Fig. 2b) and HRTEM of the calcinated powder (Fig. 2b) revealed aggregates of randomly oriented 8-100 nm-sized nanocrystals of various shapes with two families of lattice fringes of ~0.3 nm and 0.71-0.99 nm. The SAED pattern (insert in Fig. 2b) displays discrete rings and spot reflections, which were indexed according to both *m* and *t*-phase spacings. The net PEEL intensity (Fig. 2c) satisfactorily fits to the expected position of a direct band gap for $ZrO_2$ (solid curve) between 4-5 eV energy loss [2]. For the as-precipitated nanopowder (dash curve), the intensity threshold is clearly less pronounced, probably due to a number of defect states in the gap. The peaks below 30 eV are primarily associated with plasmons and interband transitions, while those above 30 eV are related to the Zr-$N_{2,3}$ edge with an onset at ~32 eV energy loss. An unresolved peak at ~7.4 eV is likely due to excitation of valence electrons into unoccupied d-states in the conduction band. The bulk plasmon at 13.4 eV for the nanocrystalline material is reduced in intensity and shifted to 14.7 eV for the as-precipitated sample. The broad peak at 25-26 eV is at least partly due to additional unexhausted collective excitation of all (16) valence electrons of O and Zr per $ZrO_2$ unit. Fingerprints of the $ZrO_2$ band structure in the low-loss PEEL spectra allow differentiation between the amorphous-like and nanocrystalline powders. Stabilization of the *t*-phase with much larger

crystallite sizes (10-100 nm, which is 3-10 times larger than previously reported values [3]) in spherical $ZrO_2$ particles is likely due to a strain-induced size confinement from surrounding growing crystallites and definitely not due to the presence of *m*-phase, because this phase was not observed. Since the sub-micron particles were filled with many differently oriented *t*-phase grains, it is possible that strain-induced growth limitations within the dense particles may effectively suppress the volume expansion associated with the martensitic *t*-*m* phase transformation. The $ZrO_2$ nanopowder synthesized with a high R-value consisted of loose particle agglomerates that could not suppress the *t*-*m* phase transformation. Partial stabilization of the metastable *t*-phase in this case may be due to a crystallite size effect and/or to the simultaneous presence of *m*-phase [4].

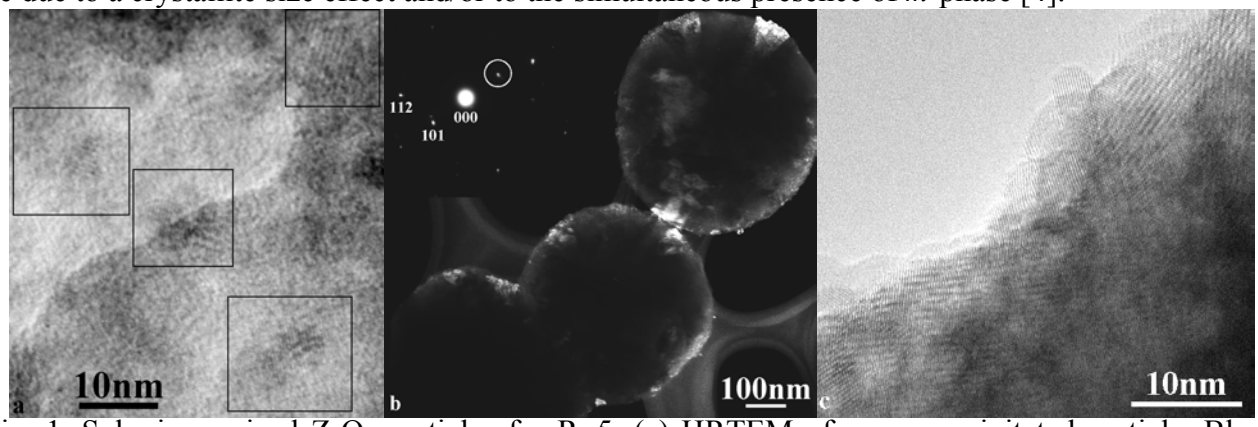


Fig. 1. Submicron-sized $ZrO_2$ particles for R=5: (a) HRTEM of an as-precipitated particle. Black rectangles enclose barely visible nanocrystallites embedded in the surrounding amorphous material. (b) DF-TEM using the $\bar{1}0\bar{1}$ reflection (indicated by the white circle in the SAED pattern, insert). (c) HRTEM showing the surface morphology and lattice fringes in a calcinated particle.

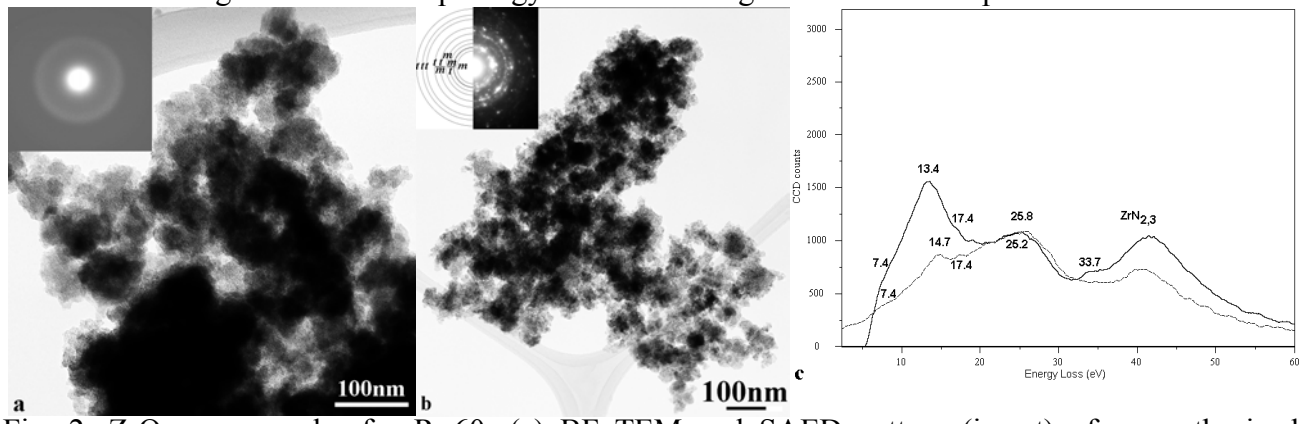


Fig. 2. $ZrO_2$ nanopowder for R=60: (a) BF TEM and SAED pattern (insert) of as-synthesized nanoparticles. (b) BF TEM and SAED pattern (insert) of *t*+*m* $ZrO_2$ nanocrystals grown after calcination. (c) PEELS single-scattering distributions derived by Fourier-log deconvolution: as-precipitated particles (dashed line) and the calcinated sample (solid line). The zero-loss peak was subtracted and the spectra were normalized by the intensity of the band at 25.2-25.8 eV.

**References**

[1] L. Ping L et al., J. Amer. Ceram. Soc. 77 (1994) 118. [2] D.W. McComb, Phys. Rev. B 54 (1996) 7094. [3] R. Nitsche et al., Nanostruct. Mater. 7 (1996) 535. [4] This research was supported by the Division of Materials Science & Engineering, Office of Science, US Department of Energy (Grant No DE-FG02-01ER45918) and by the US NSF (Grant EEC-0136710).

https://doi.org/10.1017/S1431927603442050 Published online by Cambridge University Press